Effect of the interface layer vibration modes in enhancing thermal conductivity of nanofluids

Ilyes Mitiche,[1] Omar Lamrous,[1] Said Makhlouf,[2] Francesca Marchetti,[3,4] and Nadhira Laidani[3]
[1]*Laboratoire de Physique et Chimie Quantique, Mouloud Mammeri University of Tizi-Ouzou, BP 17 RP, 15000 Tizi-Ouzou, Algeria*
[2]*Laboratoire de Mécanique, Structure et Énergétique, Mouloud Mammeri University of Tizi-Ouzou, BP 17 RP, 15000 Tizi-Ouzou, Algeria*
[3]*Center for Materials and Microsystems, Fondazione Bruno Kessler, Via Sommariva 18, 38123 Povo, Trento, Italy*
[4]*Department of Physics, University of Trento, Via Sommariva 15, 38123 Povo, Trento, Italy*

(Received 28 May 2019; published 16 October 2019)

The present paper reports on an investigation of the effect of the interface layers in enhancing thermal conductivity of Cu-Ar nanofluids. The approach is based on linear response theory combined with equilibrium molecular dynamics simulations. For a wettability parameter of 1.4 and volume fraction of 5.8%, simulation results show enhancements in thermal conductivity as high as 50%. Among others, the most salient result concerns the contribution of the vibration modes of liquid Ar atoms around Cu nanoparticles (NPs) in enhancing thermal conductivity of the nanofluid. Our findings reveal that these vibration modes coincide on a large domain of frequencies ($10 - 50\,\mathrm{ps}^{-1}$) with those of Cu atoms of the NPs. The enhancement of the thermal conductivity was explained by the increase of vibrational mean-free paths.

DOI: 10.1103/PhysRevE.100.042120

I. INTRODUCTION

Nanofluids consist of insoluble nanosized solid particles immersed in liquids. They are found in natural living cells and can also be artificially produced in the laboratory for chemical, biological, and thermal transport applications. This last position is of particular interest in this paper that it concerns the investigation of the dependence of the thermal transport across nanoparticle-fluid interfaces. According to the literature, it has been revealed that the enhancement of the thermal conductivity observed in nanofluids may be attributed to four main mechanisms: Brownian motion of the nanoparticles (NPs) [1–3], NPs forming clusters [4,5], the formation of interface layers [1,6,7], and the nature of heat transport in the NPs [1]. If it is established that the formation of interface layers is the most quoted mechanism [1,7–11], its contribution in enhancing thermal conductivity is still debated by researchers. Eapen *et al.* [10,12] using equilibrium molecular dynamics (EMD) simulations note that a strong cross attraction between the NPs and fluid atoms can induce a higher density of fluid atoms around the NPs allowing excess potential energies, which have an effect of additional thermal conduction processes through a potential energy exchange or a phonon collision mechanism. Sachdeva *et al.* [9], also with EMD simulations, concluded that improving the attractive interaction between NPs and the fluid induces an increase in thermal conductivity. They supposed that this is due to a reduction of Kapitza resistance between the NPs and the fluid. Tascini *et al.* [13] considering nonequilibrium molecular dynamic simulations (NEMD) showed that Kapitza resistance decreases with wettability. Mirmohammadi *et al.* [14] recently proposed EMD simulations and reported that the thermal conductivity increases with function of the surface to the volume ratio on the NPs. Liang *et al.* [11] proposed NEMD simulations in order to determine the width and the thermal conductivity of the interface layer. A width of an order of 1 nm and a thermal conductivity of 1.6 to 2.5 times higher than that of the base fluid were obtained. Then, by incorporating these results into the effective medium theory model, they assumed that the contribution of the interfacial layer to the thermal conductivity is useful only if there are clusters of particles in the fluid. Additionally, Frank *et al.* [15] using EMD simulations demonstrated how the thermal conductivity of a copper (Cu)-argon (Ar) nanofluid confined in nanochannels increases. They provide theoretical evidence concerning the organized liquid structures forming around the NP and reported the effect of the interface layer thickness. In addition, in a separate study [16], they proposed a molecular model consisting of liquid Ar confined by two ideal parallel solid surfaces, highlighting the role of confinement in the introduction of additional transverse oscillations. Furthermore, it should be emphasized that classical approaches [15] offer an approximate representation of transport phenomena at nanoscale, leading to inaccurate and sometimes incorrect predictions. However, the understanding of thermal transport of nanofluidic systems was considered as an atomic-scale process. Consequently, a variety of studies were realized to identify and quantify the main mechanisms that govern heat transport at a solid-liquid interface.

In this present work, we are interested in the fluid layer of the NP-fluid interface by studying its dynamic properties while highlighting the effect on thermal conductivity. For this, in the framework of the linear response theory (Green-Kubo formalism), we first performed EMD simulations to determine these transport properties in the case of Cu-Ar nanofluid. Then the impact of the interface on the thermal conductivity is discussed.

II. THEORETICAL PROTOCOL

All calculations were performed at the linear response theory level associated with EMD simulations to predict

 ©2019 American Physical Society

the effect of Cu NPs on thermal conductivity of Ar liquid. Therefore, the Green-Kubo relation allows us to calculate the effective thermal conductivity k as [17,18]

$$k = \frac{1}{3Vk_BT^2}\int_0^{+\infty}\langle \mathbf{J}_q(t)\mathbf{J}_q(0)\rangle\, dt, \quad (1)$$

where V and T are the volume and the temperature of the system, respectively, and k_B denotes the Boltzmann constant. The form of $C_{hh}(t) = \langle \mathbf{J}_q(t)\mathbf{J}_q(0)\rangle$ gives the heat current autocorrelation function (HACF). The instantaneous microscopic heat flux $\mathbf{J}_q$ for a multicomponent system is calculated using the following equation [17,18]:

$$\mathbf{J}_q = \sum_i^N e_i\mathbf{v}_i + \frac{1}{2}\sum_i^N\sum_{j\neq i}^N \mathbf{r}_{ij}(\mathbf{F}_{ij}\cdot\mathbf{v}_i) - \sum_i^N h_\alpha\mathbf{v}_i, \quad (2)$$

where e_i is the internal energy, which includes the kinetic and potential energy of each atom i, $\mathbf{F}_{ij}$ is the force on atom i due to the j one from the potential, and h_α is the mean partial enthalpy of each species α, which is calculated as the sum of the average kinetic energy, potential energy, and collision [12].

To carry out a realistic simulation of heat conduction, we considered a system consisting of a cubic box containing eight solid Cu NPs with a 2.7 nm diameter dispersed into liquid Ar. This system was built as follows. We first drew a cubic-face-centered (CFC) structure with every site occupied by Ar at an initial density of 1418 kg/m^3. Then we created eight spherical cavities filled with the Cu NPs. These NPs therefore contained a finite number of atoms in a CFC lattice at density of 8950 kg/m^3. This means that the NPs' volume fraction could be varied according to the volume of the system. The periodic boundary conditions were used in three dimensions. Note that the presence of additional particles impedes the development of artificial self-correlations [19]. In this context, the number of eight NPs is chosen to alleviate this artifact while satisfying the convergence test.

We started the simulation by a first equilibration step in an NVT ensemble using a Nosé-Hoover chain thermostat [20,21] at temperature $T = 86$ K for 10^5 time steps. This was followed by 3×10^5 time steps in an NPT ensemble at the same temperature and at 1 atm pressure using the Matryna *et al.* method [21–23]. In order to forget the influence of the barostat on the system, the equilibration in an NVT ensemble was continued for 10^5 time steps. Finally, we finished the equilibration in an NVE ensemble for 10^5 time steps to forget the influence of the thermostat. Then, the thermal conductivity was computed in 10^6 times steps in an NVE ensemble and averaged over 12 independent runs for additional phase-space sampling. The time step is $\delta t = 2$ fs. All the simulations were performed with home-made molecular dynamics code. See Appendix A for more details on the interaction potential used.

We realized the simulations for various volume fractions of NPs. This was done by varying the initial volume of the simulation box using the same number of NPs and initial densities of Cu and Ar. It should be noted that the volume fraction was calculated using the box volume and the densities of Cu and Ar obtained after the equilibration steps. We studied the influence of the wettability between the fluid and the NPs by tuning the Lennard-Jones interaction potential attractive part between Ag and Cu atoms (see Appendix A).

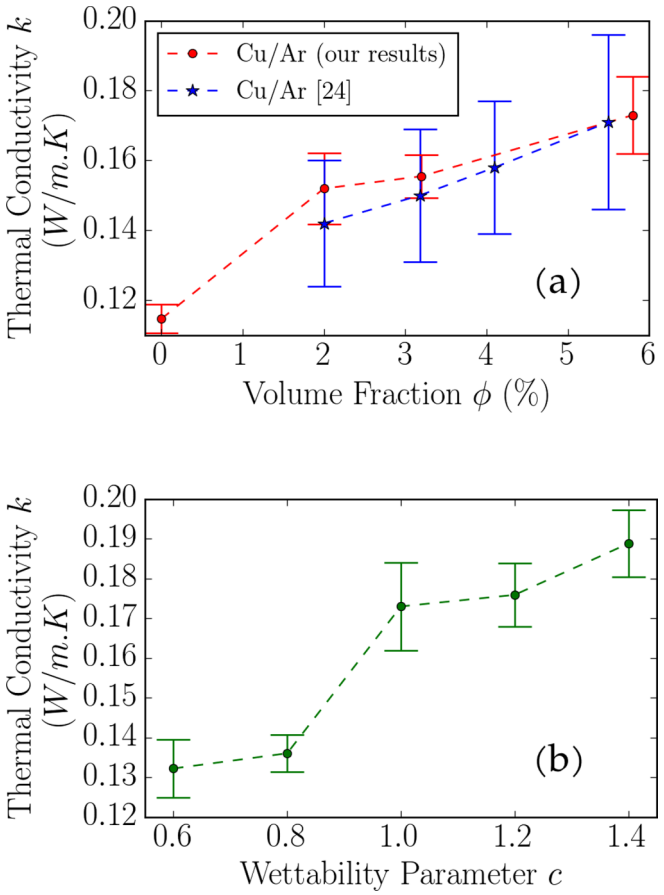

FIG. 1. Thermal conductivity as function of (a) volume fraction, ϕ (with $c = 1$) and (b) wettability parameter, c (with $\phi = 5.8\%$).

III. RESULTS

Figure 1(a) shows the predicted variation of the effective thermal conductivity of the nanofluid, k, with the volume fraction, ϕ, over the range 0%–5.8%. Over ϕ, there was a remarkable increase of k, which is in good agreement with the value fromf the literature [24]. We observe that the value of k calculated for the pure Ar case (0.114 W/m · K) is close to the experimental value (0.121 W/m · K) obtained at the normal boiling point [25]. With the exception of the first point ($\phi = 0$) and considering the error bars, the results clearly show that k against ϕ is governed by a linear relationship, as seen in previous studies [9,12,19]. A second result reported in Fig. 1(b) also shows that k increases as the wettability parameter, c, is increased, which is consistent with that obtained in Ref. [9]. Therefore, the wettability parameter has a large influence on the value of the effective thermal conductivity of the nanofluid.

This led to us to discuss this issue in the case of a Cu-Ar nanofluid. The density of the Ar atoms for different values of ϕ versus the distance with respect to the center of mass of the NPs, r, is depicted in Fig. 2(a). At the lowest values of r, from 1.4 to 1.9 nm for all ϕ values, 2%, 3.2%, and 5.8%, the distribution density of liquid atoms exhibits two

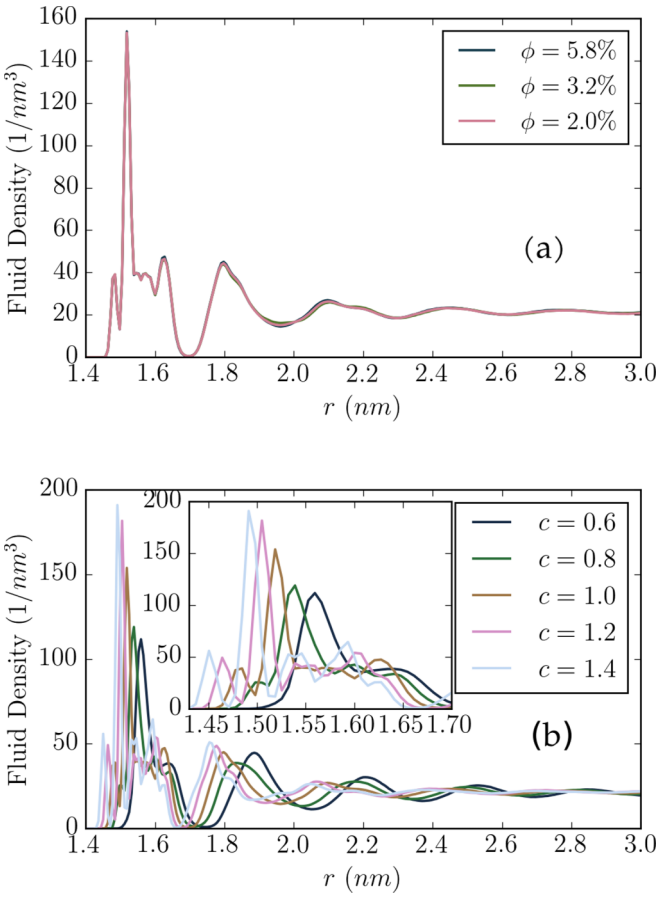

FIG. 2. Density of Ar atoms versus the distance with respect to the mass center of the Cu NPs for (a) different volume fractions, ϕ and $c = 1$, and (b) different wettability parameters, c and $\phi = 5.8\%$.

noticeable peaks corresponding to the presence of the layer of Ar bearing a resemblance to the ordered crystalline structure. As we can see, the density of Ar is high near the surface of the NPs, which agrees well with the observation made in Ref. [13]. Beyond 2.8 nm, the density returns to an almost constant value, which corresponds to the density of the Ar liquid. Moreover, we found that the intensity and the position of the peaks remained constant with ϕ. However, they were very dependent on c as illustrated in Fig. 2(b). As c increases, the liquid density around the NPs increases, and the position of the peaks get closer to the surface of the NPs. This is due to the attractive part of the interaction potential, which becomes more important.

To study the dynamics behavior of the Ar atoms, we used the spectrum of the velocity autocorrelation function (VACF) given as follows [21,26]:

$$C_{vv}(\omega) = \frac{1}{3}\int_{-\infty}^{\infty} \mathbf{v}(t)\cdot\mathbf{v}(0)\exp(-i\omega t)\,d\omega. \qquad (3)$$

The computing method of the VACF spectrum is given in Appendix B.

The VACF spectrum is analogous to the phonon density of states for a harmonic solid [18]. Therefore, C_{vv} provides information on atomic vibrations. However, for a liquid, C_{vv} contains information on the vibrations and the atomic

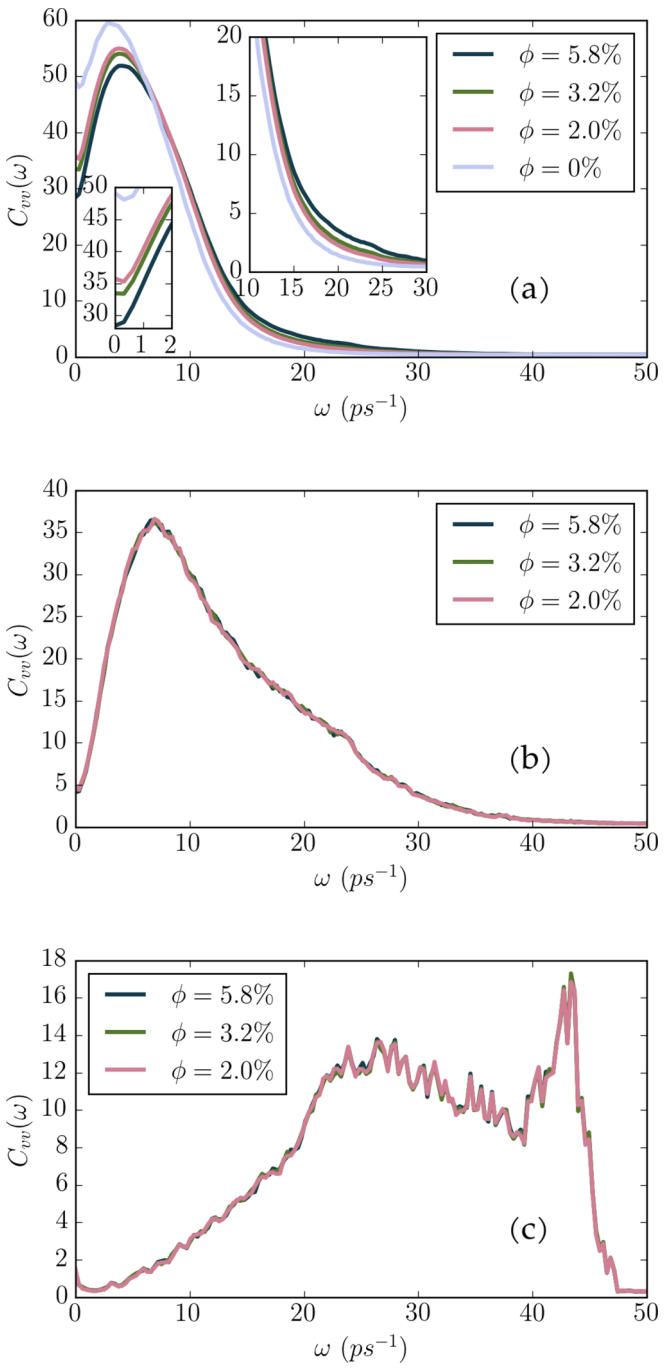

FIG. 3. The mean VACF spectra of (a) all Ar liquid atoms, (b) Ar atoms which are at a distance less than 5 nm from the center of mass of the Cu NPs, and (c) Cu atoms for different values of ϕ and $c = 1.0$.

diffusion. The contribution of diffusion to C_{vv} corresponds to $C_{vv}(\omega = 0)$, which is proportional to the diffusion constant [27].

Figure 3(a) depicts the predicted mean VACF spectra of the all Ar atoms calculated for different values of ϕ. When ϕ increases, the diffusion constant $[C_{vv}(\omega = 0)]$ decreases on one hand, and on the other hand the vibrational spectrum is slightly raised from $\omega = 10$ ps^{-1}, which means that the presence of NPs hinders the diffusion and promotes high-frequency vibrations. This behavior became more important

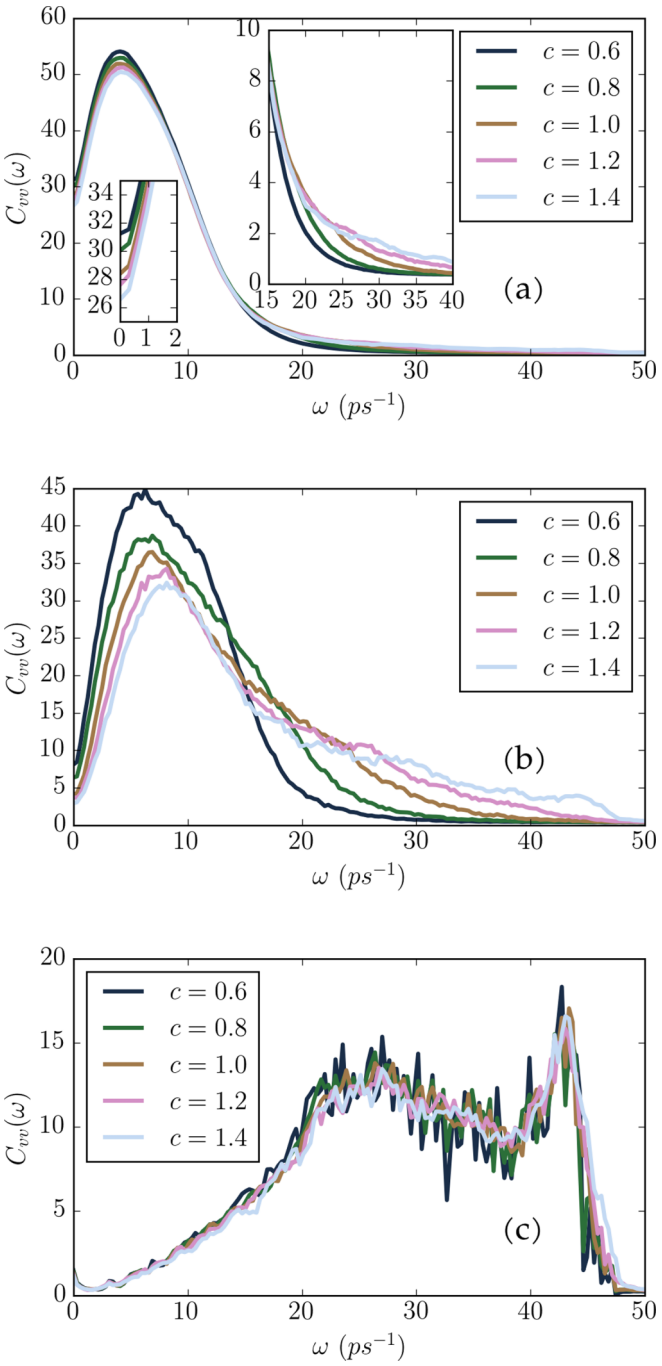

FIG. 4. The mean VACF spectra of (a) all Ar liquid atoms, (b) Ar atoms which are at a distance less of 5 nm from the center of mass of the Cu NPs, and (c) Cu atoms for different values of the c parameter and $\phi = 5.8\%$.

when approaching the Cu NPs as shown in Fig. 3(b). When calculating the mean VACF spectrum of the Ar atoms located at a distance greater than 5 nm from the center of mass of the NPs (figure not shown), there is a decrease in the density of vibration modes with a frequency greater than 10 ps^{-1} compared to that corresponding to the mean VACF spectrum of all Ar atoms of the nanofluid [Fig. 3(a)], which would mean that the high-frequency vibration modes were localized around the Cu NPs. Figure 3(c) depicts the mean VACF spectrum of Cu atoms for different values of ϕ, which presents a similar shape to that of the Cu phonon density of states [28–30]. However, we have a finite value of $C_{vv}(\omega = 0)$ due to the NPs' diffusion in the fluid. The spectrum of the Ar atoms around the Cu NPs presents a good overlap with the spectrum of the Cu NPs. This may ensure a better heat exchange through the interface between the Cu NPs and Ar liquid [13,31,32]. As can be seen in Figs. 3(b) and 3(c), ϕ has no effect on the average spectra relating to the Ar atoms around the NPs and the Cu atoms. The change of the spectrum of Ar as a function of ϕ is due to the fact that when ϕ increases, the volume fraction of the interface layer increases and thus allows one to see the contribution of the vibration modes of the interface layer. However, as shown in Fig. 4, the VACF spectra are sensitive to the c parameter, i.e., to the interaction between the Cu NPs and the Ar atoms. Figure 4(a) corresponding to the mean VACF spectrum of all Ar atoms shows that the higher c is set, the more high-frequency vibration modes are boosted. This behavior finds its explanation in the creation of these localized modes around Cu NPs, as can be seen in Fig. 4(b). Similarly, the spectrum of the Ar atoms around the Cu NPs presents a good overlap with the spectrum of the Cu NPs [see Fig. 4(c)]; however, this overlap becomes more important when c is higher, which can cause a better heat exchange.

Figure 5 shows for different values of c the spectrum of HACF of the nanofluid $C_{hh}(\omega)$] compared to the mean VACF vibration spectrum of Cu and Ar atoms around Cu NPs. The HACF spectrum presents a high-intensity region with a frequency range 10–50 ps^{-1}, which does not appear in the HACF spectrum of the Ar liquid, depicted in Fig. 6. This region corresponds to the frequency domain of the vibration modes of Cu atoms. As mentioned above, the overlap between the VACF spectrum of Ar atoms around the Cu NPs and Cu atoms of NPs becomes more important as c is high, and the intensity of the HACF spectrum as a function of frequency increases with this overlap (see Fig. 5). We can conclude that the vibration modes of Cu contribute more to the thermal conductivity of the nanofluid when c increases. This result can be explained by an enhancement of the mean-free path of these vibration modes created in the liquid around the Cu NPs [33]. In summary, it can be said that the Ar layer around the NPs contributes effectively in enhancing thermal conductivity of the nanofluid.

IV. SUMMARY

In this paper we have studied the effect of the volume fraction and te wettability on the thermal conductivity of nanofluid using EMD simulations. We have focused on the role of the interface layer in enhancing thermal conductivity, which is an issue that to our knowledge has not been investigated sufficiently.

We have shown that the thermal conductivity of the nanofluid increases significantly both with the volume fraction of the NPs and with the wettability parameter. The mean VACF spectrum of the Ar atoms around the Cu NPs presents a good overlap with the spectrum of the Cu NPs, and this overlap is more important when wettability parameter is high, which can result in high contribution of the Cu vibration

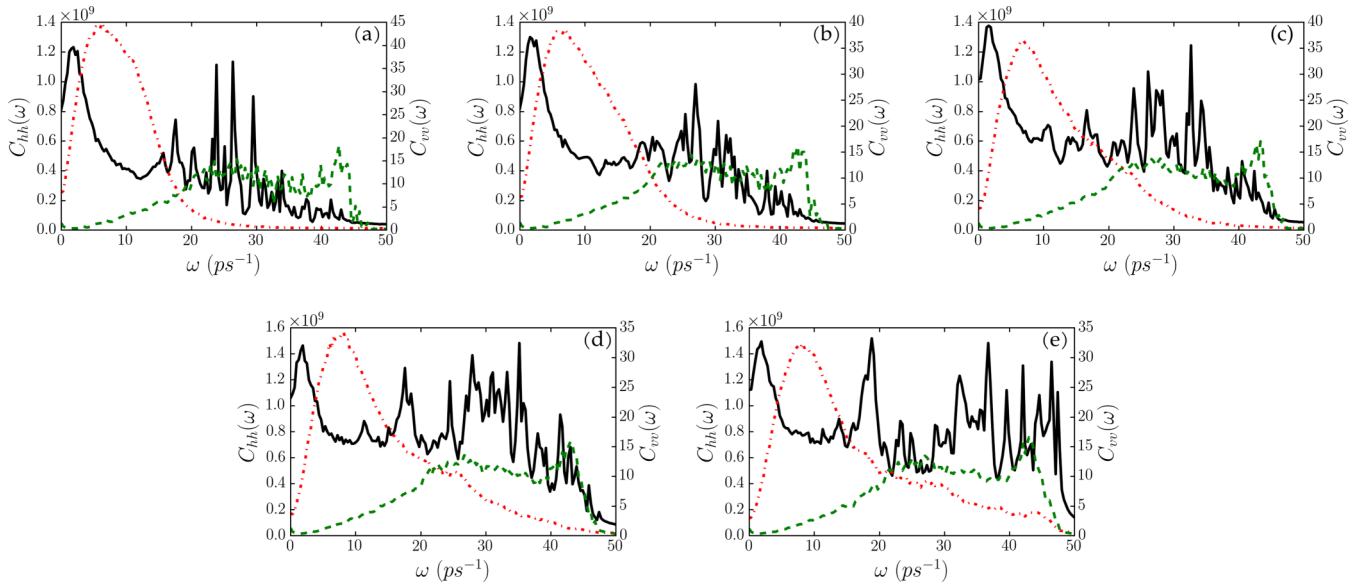

FIG. 5. The HACF spectrum (solid black line) compared to the mean VACF spectra of Ar atoms, which is at a distance less of 5 nm from the center of mass of the Cu NPs (dash-dot red line) and Cu atoms (dashed green line) for different c parameters: (a) $c = 0.6$, (b) $c = 0.8$, (c) $c = 1.0$, (d) $c = 1.2$, and (e) $c = 1.4$, with $\phi = 5.8\%$.

modes on the thermal conductivity. New experimental work and simulations will be welcome to compare our results, as well as to improve our theoretical protocol. Replacing Ar with water is an interesting study that will be done in the future to optimize the efficiency of a solar distiller, but this requires a substantial modification of the theoretical protocol, such as consideration of the electrical charge on the surface of the NPs [34].

ACKNOWLEDGMENTS

Support for this work from the Ministère Algérien de l'Enseignement Supérieur et de la Recherche Scientifique and the Italian Ministero degli Affari Esteri e della Cooperazione Internazionale, Direzione Generale per la Promozione del Sistema Paese for the bilateral Algeria-Italy project under Grant No. PGR00858 is acknowledged.

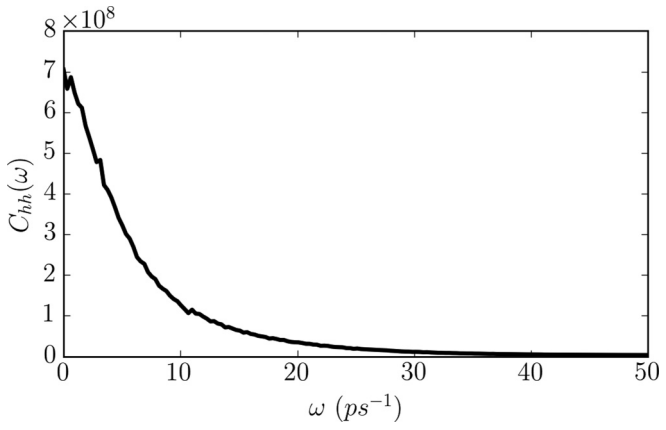

FIG. 6. The HACF spectrum of Ar fluid without Cu NPs.

APPENDIX A: INTERACTIONS POTENTIALS

The interatomic interaction between Ar-Ar atoms and Ar-Cu was taken to be of the Lennard-Jones (LJ) form, with parameters $\varepsilon_{\mathrm{Ar-Ar}} = 1.67 \times 10^{-21}$ J, $\sigma_{\mathrm{Ar-Ar}} = 0.3405$ nm, $\varepsilon_{\mathrm{Cu-Ar}} = 10.41 \times 10^{-21}$ J, and $\sigma_{\mathrm{Cu-Ar}} = 0.2872$ nm [24], with a cutoff distance $r_c = 2.8\sigma_{\mathrm{Ar-Ar}}$. To modify the wettability of Cu NPs by the liquid Ar, we multiplied the attractive part of the LJ potential by a parameter c [35]:

$$\phi(r_{ij}) = 4\epsilon_{ij}\left[\left(\frac{\sigma_{ij}}{r_{ij}}\right)^{12} - c\left(\frac{\sigma_{ij}}{r_{ij}}\right)^{6}\right]. \tag{A1}$$

In particular, strong wetting was obtained when $c > 1$. For Cu-Cu interactions, the embedded atom method potential [36] was used, which was considered in the Mendelev *et al.* parameters [37,38].

APPENDIX B: VELOCITY AUTOCORRELATION FUNCTION SPECTRA COMPUTING METHOD

To compute the VACF spectra of the three atoms types (Cu NPs, liquid Ar, and Ar interface layer atoms), we began computing the VACF of each type for a period of 10^4 time steps using the function

$$C_\alpha(t) = \frac{1}{3N_\alpha}\sum_{i=1}^{N_\alpha}\mathbf{v}_i(0)\cdot\mathbf{v}_i(t), \tag{B1}$$

where N_α was the number of atoms of each type. The final VACF was obtained by averaging throughout the MD simulations and for 12 independent runs. The list of the Ar interface layer atoms was obtained by listing all the Ar atoms located at a distance less than 5 nm from the centers of mass of Cu NPs. This list was updated every 10^4 time steps. Finally, the VACF spectrum was obtained by making a fast Fourier transform of the VACF using the Python Library Numpy.

[1] P. Keblinski, S. Phillpot, S. Choi, and J. Eastman, Mechanisms of heat flow in suspensions of nano-sized particles (nanofluids), Int. J. Heat Mass Transf. **45**, 855 (2002).

[2] S. P. Jang and S. U. Choi, Role of Brownian motion in the enhanced thermal conductivity of nanofluids, Appl. Phys. Lett. **84**, 4316 (2004).

[3] W. Evans, J. Fish, and P. Keblinski, Role of Brownian motion hydrodynamics on nanofluid thermal conductivity, Appl. Phys. Lett. **88**, 093116 (2006).

[4] R. Prasher, P. E. Phelan, and P. Bhattacharya, Effect of aggregation kinetics on the thermal conductivity of nanoscale colloidal solutions (nanofluid), Nano Lett. **6**, 1529 (2006).

[5] R. Prasher, W. Evans, P. Meakin, J. Fish, P. Phelan, and P. Keblinski, Effect of aggregation on thermal conduction in colloidal nanofluids, Appl. Phys. Lett. **89**, 143119 (2006).

[6] W. Yu and S. Choi, The role of interfacial layers in the enhanced thermal conductivity of nanofluids: A renovated Maxwell model, J. Nanopart. Res. **5**, 167 (2003).

[7] H. Xie, M. Fujii, and X. Zhang, Effect of interfacial nanolayer on the effective thermal conductivity of nanoparticle-fluid mixture, Int. J. Heat Mass Transf. **48**, 2926 (2005).

[8] P. Keblinski, R. Prasher, and J. Eapen, Thermal conductance of nanofluids: Is the controversy over? J. Nanopart. Res. **10**, 1089 (2008).

[9] P. Sachdeva and R. Kumar, Effect of hydration layer and surface wettability in enhancing thermal conductivity of nanofluids, Appl. Phys. Lett. **95**, 223105 (2009).

[10] J. Eapen, J. Li, and S. Yip, Beyond the Maxwell limit: Thermal conduction in nanofluids with percolating fluid structures, Phys. Rev. E **76**, 062501 (2007).

[11] Z. Liang and H.-L. Tsai, Thermal conductivity of interfacial layers in nanofluids, Phys. Rev. E **83**, 041602 (2011).

[12] J. Eapen, J. Li, and S. Yip, Mechanism of Thermal Transport in Dilute Nanocolloids, Phys. Rev. Lett. **98**, 028302 (2007).

[13] A. S. Tascini, J. Armstrong, E. Chiavazzo, M. Fasano, P. Asinari, and F. Bresme, Thermal transport across nanoparticle–fluid interfaces: The interplay of interfacial curvature and nanoparticle–fluid interactions, Phys. Chem. Chem. Phys. **19**, 3244 (2017).

[14] S. A. Mirmohammadi, M. Behi, Y. Gan, and L. Shen, Particle-shape-, temperature-, and concentration-dependent thermal conductivity and viscosity of nanofluids, Phys. Rev. E **99**, 043109 (2019).

[15] M. Frank, D. Drikakis, and N. Asproulis, Thermal conductivity of nanofluid in nanochannels, Microfluid. Nanofluid. **19**, 1011 (2015).

[16] M. Frank and D. Drikakis, Solid-like heat transfer in confined liquids, Microfluid. Nanofluid. **21**, 148 (2017).

[17] W. A. Steele, in *Transport Phenomena in Fluids*, edited by H. J. M. Hanley (Marcel Dekker, New York, 1969), pp. 209–312.

[18] D. A. McQuarrie, *Statistical Mechanics* (Harper & Row, New York, 1976).

[19] M. G. Muraleedharan, D. S. Sundaram, A. Henry, and V. Yang, Thermal conductivity calculation of nano-suspensions using Green–Kubo relations with reduced artificial correlations, J. Phys.: Condens. Matter **29**, 155302 (2017).

[20] G. J. Martyna, M. L. Klein, and M. Tuckerman, Nosé–Hoover chains: The canonical ensemble via continuous dynamics, J. Chem. Phys. **97**, 2635 (1992).

[21] M. P. Allen and D. J. Tildesley, *Computer Simulation of Liquids* (Oxford University Press, Oxford, 2017).

[22] G. J. Martyna, D. J. Tobias, and M. L. Klein, Constant pressure molecular dynamics algorithms, J. Chem. Phys. **101**, 4177 (1994).

[23] M. E. Tuckerman, J. Alejandre, R. López-Rendón, A. L. Jochim, and G. J. Martyna, A Liouville-operator derived measure-preserving integrator for molecular dynamics simulations in the isothermal–isobaric ensemble, J. Phys. A: Math. Gen. **39**, 5629 (2006).

[24] H. Kang, Y. Zhang, and M. Yang, Molecular dynamics simulation of thermal conductivity of Cu–Ar nanofluid using EAM potential for Cu–Cu interactions, Appl. Phys. A **103**, 1001 (2011).

[25] S.-C. Hwang, R. D. Lein, and D. A. Morgan, Noble gases, in *Kirk-Othmer Encyclopedia of Chemical Technology* (John Wiley & Sons, Hoboken, NJ, 2005).

[26] J.-P. Hansen and I. R. McDonald, *Theory of Simple Liquids: With Applications to Soft Matter* (Academic Press, New York, 2013).

[27] N. H. March and M. P. Tosi, *Introduction to Liquid State Physics* (World Scientific, New Jersey, 2002).

[28] E. H. Jacobsen, Elastic spectrum of copper from temperature-diffuse scattering of x-rays, Phys. Rev. **97**, 654 (1955).

[29] P. D. Bogdanoff, T. L. Swan-Wood, and B. Fultz, Phonon entropy of alloying and ordering of Cu-Au, Phys. Rev. B **68**, 014301 (2003).

[30] P. Reddy, K. Castelino, and A. Majumdar, Diffuse mismatch model of thermal boundary conductance using exact phonon dispersion, Appl. Phys. Lett. **87**, 211908 (2005).

[31] Z. Liang and H.-L. Tsai, Effect of molecular film thickness on thermal conduction across solid-film interfaces, Phys. Rev. E **83**, 061603 (2011).

[32] S. Shenogin, L. Xue, R. Ozisik, P. Keblinski, and D. G. Cahill, Role of thermal boundary resistance on the heat flow in carbon-nanotube composites, J. Appl. Phys. **95**, 8136 (2004).

[33] A. J. H. McGaughey and M. Kaviany, Thermal conductivity decomposition and analysis using molecular dynamics simulations. Part I. Lennard-Jones argon, Int. J. Heat Mass Transf. **47**, 1783 (2004).

[34] D. Lee, J.-W. Kim, and B. G. Kim, A new parameter to control heat transport in nanofluids: Surface charge state of the particle in suspension, J. Phys. Chem. B **110**, 4323 (2006).

[35] M. Vladkov and J.-L. Barrat, Modeling transient absorption and thermal conductivity in a simple nanofluid, Nano Lett. **6**, 1224 (2006).

[36] M. S. Daw and M. I. Baskes, Embedded-atom method: Derivation and application to impurities, surfaces, and other defects in metals, Phys. Rev. B **29**, 6443 (1984).

[37] M. Mendelev, M. Kramer, C. A. Becker, and M. Asta, Analysis of semi-empirical interatomic potentials appropriate for simulation of crystalline and liquid Al and Cu, Philos. Mag. **88**, 1723 (2008).

[38] The interactions of self-interstitials with twin boundaries, https://www.ctcms.nist.gov/potentials/2012–Mendelev-M-I–Cu.html.